Synthesis, Characterization, and Properties of Symmetrically Substituted, Ring-Opened Poly(ferrocenylalkoxy/aryloxysilanes)

Paul Nguyen, Goran Stojcevic, Kevin Kulbaba, Mark J. MacLachlan, Xiao-Hua Liu, Alan J. Lough, and Ian Manners*

Department of Chemistry, University of Toronto, 80 St. George Street, Toronto M5S 3H6, Ontario, Canada

Received February 23, 1998; Revised Manuscript Received May 22, 1998

ABSTRACT: A novel and convenient route to the first poly(ferrocenylsilanes) with alkoxy and aryloxy substituents at silicon is reported. The reaction sequence involves (i) unexpectedly facile and clean halogen replacement at the bridging atom of a readily accessible dichlorosilyl-bridged [1]ferrocenophane Fe(η-$C_5H_4)_2SiCl_2$ (**3**) by OR groups via reactions with aliphatic alcohols and phenols in the presence of an HCl acceptor and (ii) thermal or transition metal-catalyzed ring-opening polymerization of the new [1]-ferrocenophanes of structure Fe(η-$C_5H_4)_2Si(OR)_2$ (**4**). This allows the preparation of high molecular weight poly(ferrocenylsilanes) [Fe(η-$C_5H_4)_2Si(OR)_2]_n$ with side group substituents such as short chain alkoxy groups (**5a**−**5b**, R = OMe, OEt), fluorinated ethoxy groups (**5c**, R = OCH_2CF_3), long chain alkoxy groups (**5d**−**5g**, R = OBu, OHex, $OC_{12}H_{25}$, $OC_{18}H_{37}$), and aryloxy substituents (**5h**, **5i**, and **5k**, R = OPh, OPh-*p*-^{t}Bu, OPh-*p*-^{t}Bu, OPh-*p*-Ph) at silicon. The molecular structures of the [1]ferrocenophane monomers **4a** and **4j** have been studied by single-crystal X-ray diffraction, and these species possess strained structures with tilt angles between the planes of the cyclopentadienyl ligands of 18−19°. The new poly-(ferrocenylsilanes) possess a wide range of glass transition temperatures (T_g = −51° (**5e**) to 97 °C (**5k**)) and the materials with long chain (OC_{12} (**5f**) or OC_{18} (**5g**)) alkoxy groups crystallize and exhibit melt transitions (T_m) at −30 and +32 °C, respectively. Wide-angle X-ray scattering studies of **5g** suggest a lamellar structure with interdigitated side groups. Cyclic voltammetry studies of the selected poly-(ferrocenylsilanes) **5a** and **5i** show the characteristic two-wave pattern for poly(ferrocenes) with interacting iron atoms with a redox coupling ΔE = ca. 0.22 V.

Introduction

Polymers containing transition metals in the main chain are attracting growing attention as processable materials with novel physical (e.g., redox, magnetic, electrical) and chemical (e.g., catalytic and preceramic) properties.[1,2] Until recently, the development of this area has been hindered by the lack of viable synthetic routes to these materials.[2] The recent discovery of a thermal ring-opening polymerization (ROP) route to poly(ferrocenes) from strained metallocenophanes **1** (Scheme 1) provided facile access to high molecular weight metallocene-based polymers **2** with interacting metal atoms.[3−6] Subsequently, the anionic and transition metal-catalyzed ROP of [1]ferrocenophanes at ambient temperature has also been reported, which permits access to polymers with controlled architectures including block and graft copolymers.[7−10] Recent attention has focused on detailed studies of the interesting properties of the resulting poly(metallocenes) including their electrochemical, charge transport, electrochromic, and morphological (e.g., liquid crystalline) properties and their function as precursors to spin-aligned magnetic materials (including nanostructures) via oxidation or pyrolysis.[4,11−15]

At present, the substituents in most strained metallocenophanes and their corresponding ring-opened polymers are mainly limited to alkyl or aryl side groups.[4] The introduction of other types of substituents is therefore desirable and would be expected to further diversify the range of properties accessible with these materials.[16] In this paper we report a facile and versatile route to silicon-bridged [1]ferrocenophanes that possess alkoxy and aryloxy substituents at silicon

Scheme 1

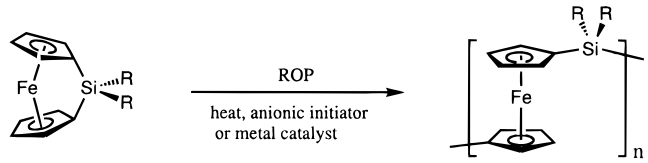

1 **2**

R = Me (**a**), Et (**b**), Bu (**c**), Hex (**d**), Ph (**e**)

and the successful ROP of these species to yield the first examples of poly(ferrocenylsilanes) with these side groups.[17]

Results and Discussion

Synthesis and NMR Characterization of the Silicon-Bridged [1]Ferrocenophanes with Alkoxy and Aryloxy Substituents at Silicon (4a−4k). The starting material was the red, crystalline dichloro-substituted silicon-bridged [1]ferrocenophane **3**, which is readily prepared in 80−90% yield via the reaction of Fe(η-$C_5H_4Li)_2$·TMEDA with $SiCl_4$, a route originally reported by Wrighton et al.[19] Although **3** is rather moisture sensitive, it can be conveniently stored prior to use under a dry, inert atmosphere for months without decomposition. Under mild conditions **3** reacts readily (25 °C, Et_2O, 3 h) with various aliphatic and aromatic alcohols in the presence of excess triethylamine via a facile nucleophilic substitution of chlorine at the bridging silicon atom (Scheme 2). The new alkoxy- or aryloxy-substituted ferrocenophanes, **4a**−**4k**, were isolated in 46−91% yields as orange-red crystalline solids

S0024-9297(98)00275-7 CCC: $15.00
Published on Web 08/19/1998

Scheme 2

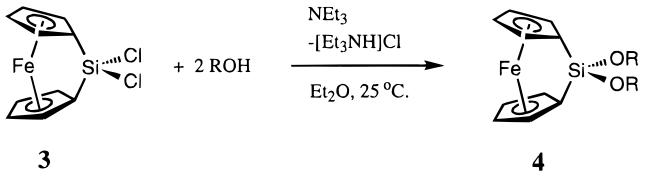

3 **4**

OR = OMe (**a**), OEt (**b**), OCH_2CF_3 (**c**), O^nBu (**d**), OHex (**e**), $OC_{12}H_{25}$ (**f**), $OC_{18}H_{37}$ (**g**), OPh (**h**), OPh-^{t}Bu (**i**) OPh-NO_2 (**j**), OPh-Ph (**k**).

by either vacuum sublimation (**4a**, **4b**) or recrystallization (**4c**, **4f**−**4k**) of the crude reaction products. Compounds **4d** and **4e** were obtained as dark red liquids from the hexane extractions of the crude mixtures that contained >98% of the desired product; the contaminants (<2%) were essentially the ring-opened species, arising from additions of the OH group across the strained Si−C bond.[19] The presence of triethylamine was found to be essential as a base to remove HCl generated in the reaction mixtrue and therefore prevent competing ring-opening reactions in the synthesis of the new alkoxy and aryloxy [1]silaferrocenophanes (**4a**−**4k**).

Compounds **4a**−**4k** were characterized by ^{1}H, ^{13}C, and ^{29}Si as well as ^{19}F (for **4c**) NMR spectroscopy and GC/MS (for **4a**, **4b**, and **4g**) as well as MS (for **4c**−**4f** and **4h**−**4k**) which provided data consistent with the assigned structures. The ^{13}C NMR spectra of **4a**−**4k** showed characteristic high-field shifts for the *ipso*-cyclopentadienyl carbon atoms bonded to silicon in the region of 34−41 ppm, consistent with the strained cyclic structure of [1]ferrocenophanes as observed previously for the alkyl and aryl analogues.[4] The ^{29}Si NMR spectra were found to be quite sensitive to the nature of the substituents showing singlet resonances for the alkoxy compounds **4a**−**4g** in the region of −29 to −35 ppm, downfield from the aryloxy derivatives in which the corresponding resonances ranged from −38 to −41 ppm. The ^{1}H NMR spectra of **4a**−**4k** showed two distinct sets of resonances for α and β hydrogens of the cyclopentadienyl ring and the expected resonances for the alkoxy and aryloxy substituents attached to silicon in the correct integrated ratio. For the trifluoroethoxy derivative (**4c**), ^{19}F NMR showed the expected triplet ($^3J_{HF}$ = 8.4 Hz) at δ 56.3 ppm relative to $CFCl_3$ in $CDCl_3$. Representative compounds (**4a**, **4b**, and **4g**) were chosen for GC/MS analyses; in all cases the resulting chromatograms showed only one peak with the corresponding molecular ions detected as the most abundant species. The remaining monomers (**4c**−**4f** and **4h**−**4k**) were analyzed using MS and showed the molecular ion as the most abundant peak.

X-ray Diffraction Studies of 4a and 4j. To study the strain present in these new [1]ferrocenophanes, single-crystal X-ray diffraction studies were performed for a selected alkoxy (**4a**, R = OMe) and aryloxy (**4j**, R = $OPhNO_2$) substituted species. Dark red crystals of **4a** suitable for X-ray diffraction studies were obtained from a high vacuum sublimation of the crude material (25 °C, 3×10^{-3} mmHg). For **4j** recrystallization from dichloromethane/hexanes (1:1) was used. The molecular structures of **4a** and **4j** are shown in Figures 1 and 2, respectively. A summary of cell constants and data collection parameters are included in Table 1. Comparative data for the present structures and other reported silicon-bridged [1]ferrocenophanes are tabulated in Table 2. In all cases the cyclopentadienyl rings are virtually planar with the mean deviations in the range of 0.001−0.005 Å from the weighted least squares planes containing C(1)−C(5) and C(6)−C(10) and are essentially eclipsed with the staggering angles of only 1.3(3)°and 0.4(4)° for **4a** and **4j**, respectively. The tilt angles of the planes of the cyclopentadienyl ligands with respect to one another are 18.6(1)° and 18.6(2)° for **4a**

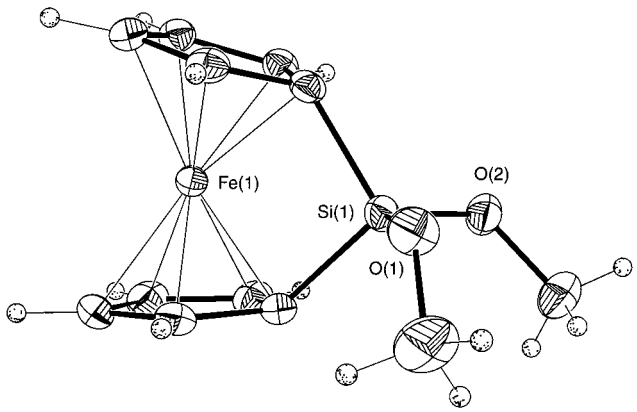

Figure 1. Molecular Structure of Fe(η-C_5H_4)$_2$Si(OMe)$_2$ (**4a**) using 50% probability thermal ellipsoids.

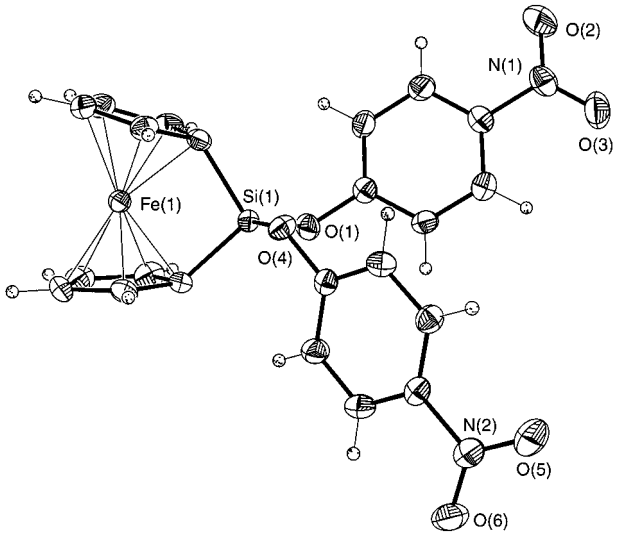

Figure 2. Molecular Structure of Fe(η-C_5H_4)$_2$Si(OPhNO_2)$_2$ (**4j**) using 50% probability thermal ellipsoids.

Table 1. Crystal Data and Structure Refinement for 4a and 4j

	4a	**4j**
empirical formula	$C_{12}H_{14}FeO_2Si$	$C_{22}H_{16}FeN_2O_6Si$
formula wt	274.17	488.31
space group	*Pbca*	*Pbca*
a (Å)	9.890(1)	16.494(6)
b (Å)	10.369(1)	14.722(4)
c (Å)	22.379(1)	16.832(4)
V (Å^3)	2294.9(5)	4087(2)
Z	8	8
D_{calcd} (Mg/m^3)	1.587	1.587
cryst size (mm)	0.55 × 0.39 × 0.33	0.48 × 0.35 × 0.31
θ range (deg)	2.75−26.99	2.72−27.01
absorption coeff (mm^{-1})	1.398	0.841
F(000)	1136	2000
data/params	2504/148	4428/289
goodness of fit	1.051	1.004
R_1 [$I > 2\sigma(I)$]	0.0272	0.0460
wR_2 (all data)	0.0784	0.1320

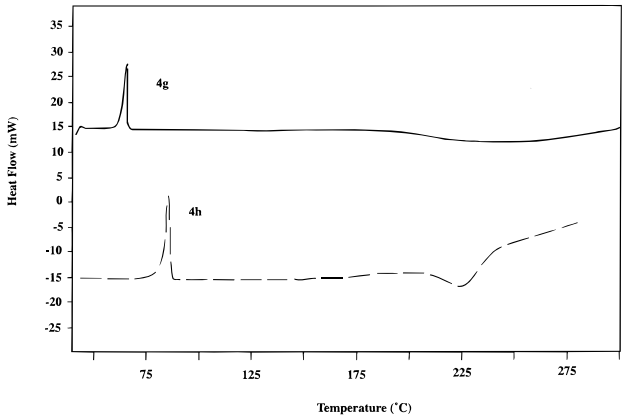

Figure 3. DSC thermograms for the silicon-bridged [1]-ferrocenophanes **4g** and **4h**.

Table 2. Comparison of Important Structural Features of Ferrocenophanes 1a, 3, 4a, and 4j

	1a	3	4a	4j
ring tilt α (deg)	20.8(5)	19.2(4)	18.6(1)	18.6(2)
Cp−Si/Cp β (deg)	37.0(6)	40.7(5)	40.0(2)	41.0(2)
Cp−Fe−Cp, δ (deg)	164.74(8)	166.5(2)	166.4(1)	166.5(1)
C_1−Si−C_6, θ (deg)	95.7(4)	100.9(2)	99.36(8)	100.49(14)
Fe displacement (Å)	0.2164(11)	0.194(4)	0.194(2)	0.193(3)
X−Si−X, (deg)	114.8(6)	111.1(1)	113.32(8)	109.52(12)
Fe- - -Si dist (Å)	2.690(3)	2.588(1)	2.6307(6)	2.6078(11)
ref	20	18	this work	this work

and **4j**, respectively. These ring-tilt angles are comparable to other silicon-bridged analogues such as the $SiCl_2$-bridged species **3** (19.2(4)°)[18] but are slightly less than in the $SiMe_2$-bridged species **1a** (20.8(5)°).[4] The values for the angle, β, between the planes of the cyclopentadienyl ligands and the C(ipso)−Si bonds are 40.0(2)° for **4a** and 41.0(2)° for **4j**, indicating large distortions from planarity at the *ipso* carbon atoms. These values are comparable to that of the dichloro derivative **3** (40.7(5)°) and are larger than the dimethyl analogue **1a** (37.0(6)°). The C_{ipso}−Si−C_{ipso} bond angles for the [1]ferrocenophanes (**3**, **4a**, and **4j**) are in the range of 99−101° and are significantly larger than that of the dimethyl derivative **1a** (95.7(4)°). The exocyclic X−Si−X bond angles for **4a** (113.32(8)°) and **4j** (109.52(12)°) are comparable to **3** (111.1(1)°). We have previously noted the significant shortening of the Fe- - -Si distance in **3** (2.588(1) Å) in comparison to the dimethyl analogue **1a** (2.690(3) Å). Similar bond-shortening effects were observed for **4a** (2.6307(6) Å) and **4j** (2.6078(11) Å).

Thermal and Transition Metal-Catalyzed ROP of [1]Ferrocenophanes. (a) Thermal ROP. To probe the ROP behavior of **4a**−**4k** each compound was initially studied by differential scanning calorimetry (DSC) at a heating rate of 10 °C/min under N_2. The DSC thermograms for **4g** and **4h** are shown in Figure 3; in each case (except for **4j**, vide infra) a sharp melting endotherm was detected followed by a broad exotherm associated with the ROP process. The onset temperatures ranged from 156 to 241 °C for the [1]ferrocenophanes containing alkoxy substituents at silicon **4a**−**4g**. The corresponding onset temperature for ROP for the aryloxy derivatives (**4h**−**4i** and **4k**) was found to increase upon incorporation of substituents at the *para* position on the phenyl ring in the order **4h** (212 °C) < **4i** (232 °C) < **4k** (263 °C) (Table 3). Compound **4j** was found to behave quite differently, showing a melt endotherm at 171 °C followed immediately by a rapid

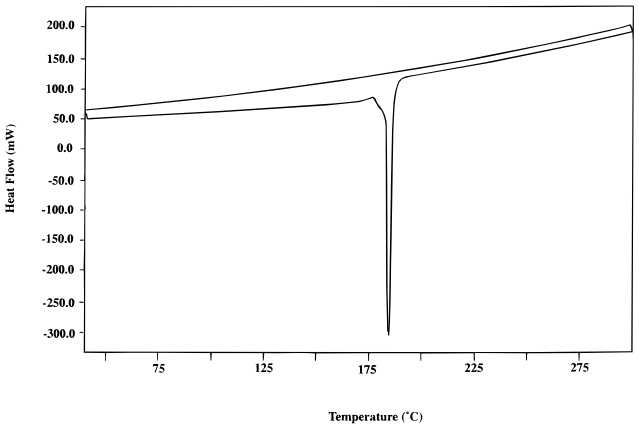

Figure 4. DSC thermogram of compound **4j**.

Scheme 3

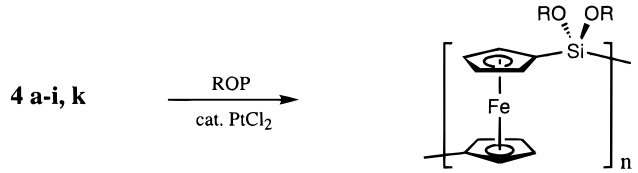

5

OR = OMe (**a**), OEt (**b**), OCH_2CF_3 (**c**), O^nBu (**d**), OHex (**e**), $OC_{12}H_{25}$ (**f**) $OC_{18}H_{37}$ (**g**), OPh (**h**), OPh-^{t}Bu (**i**), OPh-NO_2 (**j**), OPh-Ph (**k**)

decomposition exotherm at ca. 183 °C with a ΔH_{dec} of −338 kJ/mol (Figure 4). Larger scale thermal ROP reactions for **4a**−**4i** and **4k** were performed in sealed, evacuated glass tubes at elevated temperatures.

(b) $PtCl_2$-Catalyzed ROP of Monomers 4a−4i and 4k. The cyclic monomers, **4a**−**4i** and **4k,** which form dark red solutions in THF, were found to undergo transition metal-catalyzed ROP with $PtCl_2$ at 25 °C in 3 h to give viscous, light orange solutions (Scheme 3). Precipitation into methanol (hexanes can also be used for **5a**) afforded the corresponding poly(ferrocenylsilanes) **5a**−**5i** and **5k** in good isolated yields (65−88%).

(c) Structural Characterization of the Poly(ferrocenylsilanes) 5a−5i and 5k. Polymers **5a**−**5f** were obtained as orange-red gums, whereas **5g**−**5i** and **5k** were isolated as amber fibrous solids. The poly(ferrocenes) were soluble in common organic solvents such as THF, benzene (except for **5c**), and chloroform. The new polymers possessed high number average molecular weights (M_n) of *ca.* 10^5 by gel permeation chromatography (GPC) using polystyrene standards (Table 4).

Poly(ferrocenylsilanes) **5a**−**5i** and **5k** were structurally characterized by solution ^1H, ^{13}C, and ^{29}Si as well as ^{19}F (for **5c**) NMR spectroscopy, and by elemental analysis for **5a** and **5h**. The ^{29}Si NMR (Table 4) resonances are in the range of δ −13.8 to −20.9 ppm for the alkoxy polymers **5a**−**5g** and −23.8 to −24.8 ppm for the aryloxy derivatives **5h**, **5i**, and **5k**. These values are shifted downfield (ca. 14 ppm for **5a**−**5g** and 17 ppm for **5h**, **5i**, and **5k**) relative to those of the corresponding strained silicon-bridged [1]ferrocenophane precursors (δ = −29.0 to −40.8 ppm). This is in contrast to the alkyl

Table 3. Melting Onsets and Thermal ROP Onsets for 4a−4k

R	mp (°C)	thermal ROP onset (°C)
OMe (**4a**)	34	194
OEt (**4b**)	38	173
OCH_2CF_3 (**4c**)	56	200
OBu (**4d**)		156
OHex (**4e**)		241
$O(CH_2)_{11}CH_3$ (**4f**)	39	212
$O(CH_2)_{17}CH_3$ (**4g**)	63	197
OPh (**4h**)	83	212
OC_6H_4-*p*-^{t}Bu (**4i**)	111	232
OC_6H_4-*p*-NO_2 (**4j**)	171	
OC_6H_4-*p*-Ph (**4k**)	127	263

Table 4. ^{29}Si NMR Spectroscopic, Molecular Weight, Glass, and Melt Transition Data for Poly(ferrocenylsilanes) 5a−5i and 5k

R	δ^{29}Si[a]	$10^{-5}M_w$[b]	M_n[b]	PDI	T_g (T_m)/°C
OMe (**5a**)	−17.2	2.9	1.5×10^5	1.9	19
OEt (**5b**)	−20.9	8.1	3.8×10^5	2.1	0
OCH_2CF_3 (**5c**)	−13.8[d]	2.6	2.2×10^5	1.2	16
OBu (**5d**)	−20.9	8.3	3.9×10^5	2.1	−43
OHex (**5e**)	−20.5	2.2	0.9×10^5	2.4	−51
$O(CH_2)_{11}CH_3$ (**5f**)	−20.4	4.7	1.9×10^5	2.5	(−30)[c]
$O(CH_2)_{17}CH_3$ (**5g**)	−20.5	5.0	2.3×10^5	2.2	(32)[c]
OC_6H_5 (**5h**)	−24.2	4.5	2.3×10^5	2.0	54
OC_6H_4-*p*-^{t}Bu (**5i**)	−24.8	3.7	1.9×10^5	1.9	89
OC_6H_4-*p*-Ph (**5k**)	−23.8	1.3	5.4×10^4	2.4	97

[a] C_6D_6 as solvent. [b] Determined by GPC in THF using polystyrene standards [c] T_g was not detected for polymers **5f** and **5g**. [d] $CDCl_3$ as solvent.

analogues in which ^{29}Si NMR resonances for the polymers were found to be shifted upfield relative to the corresponding strained monomers. Similarly, the ^{13}C NMR *ipso* carbon resonances of polymers **5a**−**5i** and **5k** showed a downfield shift to more conventional values of 63−67 ppm compared to those of the monomers **4a**−**4i** and **4k** (37−41 ppm). The ^{1}H NMR spectra of **5a**−**5i** and **5k** were consistent with the assigned structures and showed the expected integration ratios. The ^{19}F NMR spectrum of **5c** showed a broad signal at δ 56.2 ppm relative to $CFCl_3$ in $CDCl_3$.

(d) Thermal Transition Behavior and Morphology of Poly(ferrocenylsilanes) 5a−5i and 5k. To examine the conformational flexibility of the new poly(ferrocenylsilanes) **5a**−**5i** and **5k**, their thermal transition behavior was investigated by differential scanning calorimetry (DSC). The glass transition temperatures (T_g) determined for **5a**−**5i** and **5k** are compiled in Table 4. As expected, the T_g values decrease as the length of the organic side group increases from 19 °C for **5a** (R = OMe) to 0 °C for **5b** (R = OEt) to −43 °C for **5d** (R = OBu) and to −51 °C for **5e** (R = OHex). It is of significant interest to compare the T_g values of these new poly(ferrocenylalkoxysilanes) to those of the alkyl derivatives **2a** (33 °C, R = Me), **2b** (22 °C, R = Et), **2c** (3 °C, R = Bu), and **2d** (−26 °C, R = Hex). It is clear that incorporation of a flexible Si−O spacer into the polymer side chain results in a significant lowering of the polymer glass transition temperatures. Replacing methyl groups in **5b** for CF_3 substituents as in **5c** (R = OCH_2CF_3) raised the T_g value from 0 to 16 °C. Side chain crystallization was observed when long alkoxy substituents were present in polymers **5f** (R = $OC_{12}H_{25}$) and **5g** (R = $OC_{18}H_{37}$). Thus, DSC thermograms of these materials (Figure 5) exhibited sharp melting endotherms (T_m's) at −30 °C for **5f** and 32 °C for **5g** on the heating scan, and recrystallization at −37 °C for **5f** and 27 °C for **5g** on the cooling scan. No apparent glass transitions were observed for **5f** and **5g**.

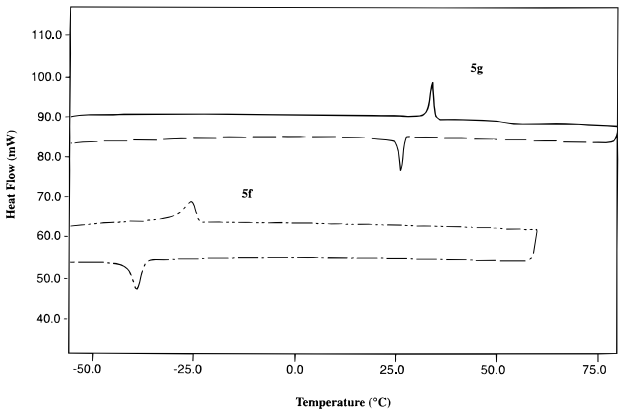

Figure 5. DSC thermograms of polymers **5f** and **5g**.

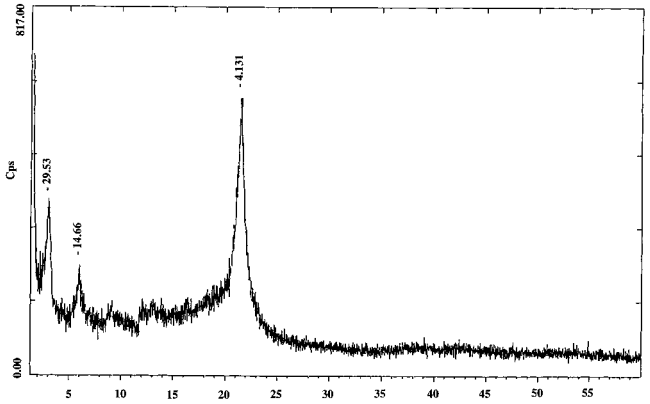

Figure 6. WAXS pattern for polymer **5g** at 25 °C.

As expected, higher T_g values were observed for the aryloxy derivatives **5h** (54 °C), **5i** (89 °C), and **5k** (97 °C) due to the steric bulk and rigidity of the phenyl moiety. In addition, a noticeable improvement in solubility was found for **5h**, which dissolved readily in THF, compared to the diphenyl analogue, **2e**, which is insoluble.

The morphology of polymers **5g**, **5i**, and **5k** were further investigated by a wide-angle X-ray scattering (WAXS) study and polarizing microscopy. Polymers **5i** and **5k** were amorphous by WAXS. On the other hand, polymer **5g** proved to be semicrystalline; a diffractogram of **5g** is shown in Figure 6. In addition to low-intensity, broad amorphous halos, sharp peaks were observed at *d* spacings of 29.5, 14.7, and 4.13 Å. The first two peaks are consistent with the (100) and (200) reflections of a lamellar structure with 29.5 Å separation between the planes. Furthermore, there are weak, but sharp, diffraction peaks near 9.7 and 7.4 Å *d* spacing, which may be assigned to the (300) and (400) reflections, respectively. Given that the fully extended length of a saturated hydrocarbon chain with 18 C atoms is 24.3 Å,[21] the alkoxy chains in the microcrystalline regions are significantly interdigitated. The sharp WAXS peak near 4.13 Å is attributed to diffraction from the crystallized side chains.

The crystalline behavior of polymer **5g** was further investigated by a combination of DSC and polarized optical microscopy (POM). On heating, polymer **5g** melted at 32 °C, and this was observed by both DSC and POM. Following melting, no light transmission was observed, which indicated that an isotropic melt had

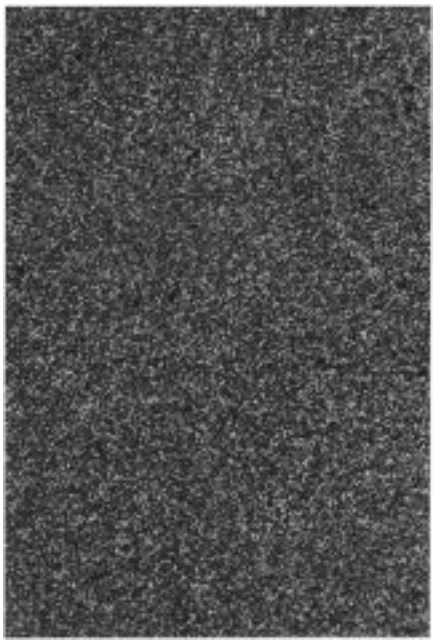

Figure 7. Crystalline phase of polymer **5g** at 24 °C under a polarizing optical microscope.

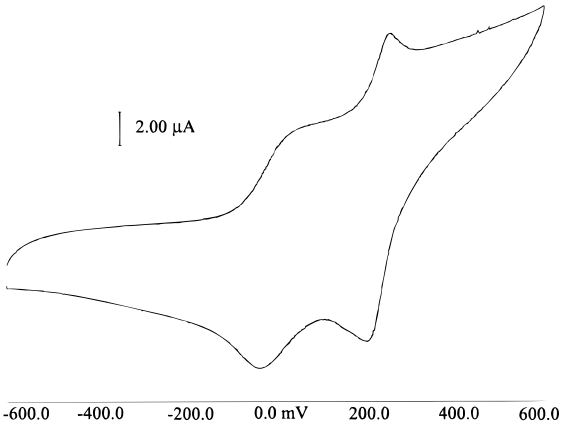

Figure 8. Cyclic voltammogram of polymer **5a** referenced to the ferrocene/ferrocenium ion couple at $E = 0.00$ mV.

formed. On cooling, the corresponding recrystallization was observed at 26 °C. The crystalline phase of polymer **5g** via POM is shown in Figure 7.

(e) Cyclic Voltammetry of Poly(ferrocenylsilanes) 5a and 5i. Poly(ferrocenylsilanes) with alkyl or aryl side groups at silicon exhibit characteristic two-wave cyclic voltammograms due to the presence of interacting metal atoms.[3,4,11a] This leads to initial oxidation at alternating iron sites followed by oxidation of those in between at a higher potential. To investigate whether the presence of alkoxy or aryloxy substituents significantly influences this behavior, the representative polymers **5a** and **5i** were studied. A cyclic voltammogram of **5a** in CH_2Cl_2 at a scan rate of 250 mV s^{-1} is shown in Figure 8. Two reversible one-electron waves were observed at $E_{1/2} = 0.01$ and 0.23 V ($\Delta E = 0.22$ V). Similar results were found for **5i** with $E_{1/2} = -0.01$ and +0.21 V ($\Delta E = 0.22$ V). These results are comparable with the two oxidation waves present in dialkyl-substituted poly(ferrocenylsilanes) reported previously ($\Delta E = 0.21-0.27$ V).[3,4,11a]

Summary

We have demonstrated a convenient and versatile synthetic route to a series of new alkoxy and aryloxy silicon-bridged [1]ferrocenophanes via a facile chlorine substitution reaction at the bridging atom of a readily available $SiCl_2$-bridged [1]ferrocenophane precursor. Thermal and transition metal-catalyzed ring-opening polymerization of these species provided access to a range of new poly(ferrocenylsilane) materials. By varying the side groups attached to silicon, elastomers with T_g values as low as −51 °C or glassy polymers with T_g values as high as 97 °C have been obtained. Polymers that exhibit side chain crystallization can also be accessed via the incorporation of long alkoxy substituents at silicon. Cyclic voltammetry showed that the metal−metal interactions are similar to those in poly(ferrocenylalkyl/arylsilanes). Further work focuses on the extension of the scope of this reaction to the related unsymmetric systems containing different substituents at silicon and detailed studies of the material properties and applications of these new poly(ferrocenes).

Experimental Section

Materials. Triethylamine, diethyl ether, THF, toluene, methanol, ethanol, 2,2,2-trifluoroethanol, *n*-butanol, and 1-dodecanol were purchased from Aldrich and were dried over sodium and distilled before use. 1-Octadecanol, phenol, 4-*tert*-butylphenol, 4-nitrophenol, and 4-phenylphenol were purchased and used as received from Aldrich.

Equipment. All reactions were carried out under an atmosphere of prepurified nitrogen using either Schlenk techniques or an inert-atmosphere glovebox, except for the purification of the polymers, which was carried out in air. Solvents were dried by standard methods, distilled, and stored under nitrogen over activated molecular sieves. Spectra (400 MHz ^{1}H NMR, 100.5 MHz ^{13}C NMR, 79.5 MHz ^{29}Si NMR, and 376.4 MHz ^{19}F NMR) were recorded on a Varian Unity 400 spectrometer. GC/MS analyses were performed on a Hewlett-Packard 5890/5971 MSD instrument equipped with a fused silica column (30 m × 0.25 mm × 0.25 mm, cross-linked 5% phenylmethyl silicone). The following conditions were used: injector, 120 °C; detector, 280 °C; oven temperature ramped from 70 to 200 °C at 10 °C/min using helium as the carrier gas. Molecular weights were estimated by gel permeation chromatography (GPC) using a Waters Associates liquid chromatograph equipped with a Model 510 HPLC pump, a Model U6K injector, Ultrastyragel columns with pore sizes of 103−105 Å, and a differential refractometer. A flow rate of 1.0 mL/min was used, and the eluent was a solution of 0.1% tetra-*n*-butylammonium bromide in THF. Polystyrene standards purchased from American Polymer Standards were used for calibration purposes.

A Perkin-Elmer DSC-7 differential scanning calorimeter equipped with a TAC 7 instrument controller was used to study the thermal behavior. The thermograms were calibrated with the melting transitions of decane and indium and were obtained at a heating rate of 10 °C/min under nitrogen.

Powder X-ray diffraction data were obtained on a Siemens D5000 diffractometer using Ni-filtered Cu Kα ($\lambda = 1.541\,78$ Å) radiation. The sample was scanned at step widths of 0.02° with 1.0 s/step in the range of 3−40° 2θ. Cyclic voltammetry of **5a** and **5i** was carried out using a PAR Model 273 potentiostat with a Pt working electrode and an Ag wire reference electrode in a Luggin capillary. All potentials are relative to the ferrocene/ferrocenium ion couple at 0.00 V, which was used as an internal reference. A 2×10^{-3} M polymer solution in freshly distilled CH_2Cl_2 with 0.1 M tetrabutylammonium hexafluorophosphate as the supporting electrolyte was used and the analyses were carried out under prepurified N_2. Polarizing optical microscopy of **5g** was carried out with a polarizing microscope equipped with a Mettler FP82 hot stage and FP80 central processor.

General Synthesis of the Silicon-Bridged [1]Ferrocenophanes 4a−4k. The dichlorosilylferrocenophane **3** was prepared by a method reported by Wrighton from the reaction of dilithioferrocene·TMEDA and $SiCl_4$.[19] The general synthesis of **4a**−**4k** is illustrated (vide infra) by the synthesis of **4a** from the reaction of **3** and the appropriate alcohol in the presence of excess Et_3N. In all cases the alcohols were used as neat liquids or in solid form and the reaction was allowed to stir at room temperature for 3 h; then the solvent was removed in vacuo. Compounds **4a** and **4b** were purified by vacuum sublimation (25 °C, 3×10^{-3} mmHg); compounds **4d** and **4e** were pure by ^{1}H NMR analysis and were used in the ring-opening polymerization experiments without further purification. Recrystallization at −30 °C was used to purify the following compounds: **4c** and **4f**−**4i** from hexanes, **4j** from toluene, and **4k** from dichloromethane/hexanes (1:1).

Synthesis of Monomer 4a. CH_3OH (0.20 mL, 4.9 mmol) was added dropwise via a syringe to a solution containing **3** (700 mg, 2.4 mmol) and Et_3N (5.6 mL, 39 mmol) in 70 mL of Et_2O under N_2. The reaction was allowed to stir at room temperature for 3 h, and then the solvent was removed in vacuo. The crude product was taken up in 50 mL of hexanes and filtered through Celite to afford a clear orange solution. Hexanes was removed in vacuo, and **4a** was obtained as red crystals (420 mg, 62% yield) by sublimation under vacuum (3×10^{-3} mmHg).

For **4a**: red-orange crystals; yield 62%; ^{1}H NMR (C_6D_6, 400 MHz) δ 3.63 (s, 6H, OCH_3), 4.14 (m, 4H, Cp), 4.40 (m, 4H, Cp) ppm; ^{13}C NMR (C_6D_6, 400 MHz), δ 39.7 (*ipso*-Cp), 50.2 (OCH_3), 75.2 (Cp), 77.9 (Cp) ppm; ^{29}Si NMR (C_6D_6, 400 MHz) δ −31.0 ppm; GC/MS (EI, 70 eV) *m*/*z* (%) 274 (M^+, 100).

For **4b**: red-orange crystals; yield 78%; ^{1}H NMR (C_6D_6) δ 1.26 (t, $^3J_{HH}$ = 7 Hz, 6H, CH_3), 4.02 (q, $^3J_{HH}$ = 7 Hz, 4H, OCH_2), 4.17 (m, 4H, Cp), 4.43 (m, 4H, Cp) ppm; ^{13}C NMR (C_6D_6) δ 18.4 (CH_3), 40.0 (*ipso*-Cp), 58.2 (OCH_2), 75.1 (Cp), 77.5 (Cp) ppm; ^{29}Si NMR (C_6D_6) δ −34.8 ppm; GC/MS (EI, 70 eV) *m*/*z* (%) 302 (M^+, 100).

For **4c**: red-orange crystals; yield 51%; ^{1}H NMR (C_6D_6) δ 3.88 (q, $^3J_{HF}$ = 8.5 Hz, 4H, OCH_2CF_3), 3.96 (m, 4H, Cp), 4.33 (m, 4H, Cp) ppm; ^{13}C NMR (C_6D_6) δ 37.1 (*ipso*-Cp), 60.3 (q, $^2J_{CF}$ = 36.3 Hz, OCH_2), 75.2 (Cp), 79.0 (Cp), 124.5 (q, $^1J_{CF}$ = 274.9 Hz, CF_3) ppm; ^{29}Si NMR (C_6D_6) δ −29.0 ppm; ^{19}F NMR ($CDCl_3$) δ 56.3 (t, $^3J_{HF}$ = 8.4 Hz, CF_3) ppm; MS (EI, 70 eV) *m*/*z* (%) 410 (M^+, 100).

For **4d**: red liquid; yield 84%; ^{1}H NMR (C_6D_6) δ 0.90 (t, $^3J_{HH}$ = 7.3 Hz, 6H, CH_3), 1.42 (m, 4H, CH_2), 1.66 (m, 4H, CH_2), 4.04 (t, $^3J_{HH}$ = 6.5 Hz, 4H, OCH_2), 4.20 (m, 4H, Cp), 4.40 (m, 4H, Cp) ppm; ^{13}C NMR (C_6D_6) δ 14.2 (CH_3), 19.6 (CH_2), 35.3 (CH_2), 41.3 (*ipso*-Cp), 62.5 (OCH_2), 75.8 (Cp), 78.1 (Cp); ^{29}Si NMR (C_6D_6) δ −34.7 ppm; MS (EI, 70 eV) *m*/*z* (%) 358 (M^+, 100).

For **4e**: red liquid; yield 91%; ^{1}H NMR (C_6D_6) δ 0.88 (t, $^3J_{HH}$ = 7.9 Hz, 6H, CH_3), 1.27 (br m, 8H, CH_2), 1.42 (m, 4H, CH_2), 1.71 (m, $^3J_{HH}$ = 7.1 Hz, 4H, CH_2), 4.07 (t, $^3J_{HH}$ = 6.6 Hz, 4H, OCH_2), 4.22 (m, 4H, Cp), 4.45 (m, 4H, Cp) ppm; ^{13}C NMR (C_6D_6) δ 14.3 (CH_3), 23.1 (CH_2), 26.0 (CH_2), 32.0 (CH_2), 33.2 (CH_2), 41.2 (*ipso*-Cp), 62.8 (OCH_2), 75.7 (Cp), 78.0 (Cp); ^{29}Si NMR (C_6D_6) δ −34.7 ppm; MS (EI, 70 eV) *m*/*z* (%): 414 (M^+, 100).

For **4f**: red-orange solid; yield 71%; ^{1}H NMR (C_6D_6) δ 0.92 (t, $^3J_{HH}$ = 6.8 Hz, 6H, CH_3), 1.31 (br m, 32H, CH_2), 1.48 (m, 4H, CH_2), 1.77 (m, $^3J_{HH}$ = 7.1 Hz, 4H, CH_2), 4.13 (t, $^3J_{HH}$ = 6.6 Hz, 4H, OCH_2), 4.25 (m, 4H, Cp), 4.45 (m, 4H, Cp) ppm; ^{13}C NMR (C_6D_6) δ 14.4 (CH_3), 23.1 (CH_2), 26.4 (CH_2), 29.8 (CH_2), 29.9 (CH_2), 30.1 (CH_2), 30.2 (CH_2), 32.3 (CH_2), 33.2 (CH_2), 41.2 (*ipso*-Cp), 62.9 (OCH_2), 75.7 (Cp), 78.0 (Cp); ^{29}Si NMR (C_6D_6) δ −34.7 ppm; MS (EI, 70 eV) *m*/*z* (%) 582 (M^+, 100).

For **4g**: red-orange solid; yield 87%; ^{1}H NMR (C_6D_6) δ 0.92 (t, $^3J_{HH}$ = 6.2 Hz, 6H, CH_3), 1.36 (br m, 56H, CH_2), 1.49 (m, 4H, CH_2), 1.77 (m, $^3J_{HH}$ = 7.0 Hz, 4H, CH_2), 4.12 (t, $^3J_{HH}$ = 6.4 Hz, 4H, OCH_2), 4.24 (m, 4H, Cp), 4.45 (m, 4H, Cp) ppm; ^{13}C NMR (C_6D_6) δ 14.3 (CH_3), 23.1 (CH_2), 26.4 (CH_2), 29.8 (CH_2), 29.9 (CH_2), 30.2 (CH_2), 32.3 (CH_2), 33.2 (CH_2), 41.3 (*ipso*-Cp), 62.9 (OCH_2), 75.8 (Cp), 78.0 (Cp); ^{29}Si NMR (C_6D_6) δ −34.6 ppm; GC/MS (EI, 70 eV) *m*/*z* (%) 750 (M^+, 100).

For **4h**: red-orange solid; yield 77%; ^{1}H NMR (C_6D_6) δ 4.15 (m, 4H, Cp), 4.35 (m, 4H, Cp), 6.83 (m, 2H, *para* phenyl H), 7.05 (m, 4H, *meta* phenyl H), 7.30 (m, 4H, *ortho* phenyl H) ppm; ^{13}C NMR (C_6D_6) δ 38.1 (*ipso*-Cp), 75.1 (Cp), 78.4 (Cp), 120.1 (*para* phenyl), 122.8 (*meta* phenyl), 129.8 (*ortho* phenyl), 153.2 (*ipso* phenyl) ppm; ^{29}Si NMR (C_6D_6) δ −40.8 ppm; MS (EI, 70 eV) *m*/*z* (%) 398 (M^+, 100).

For **4i**: red-orange solid; yield 78%; ^{1}H NMR (C_6D_6) δ 1.18 (s, 18H, CH_3), 4.23 (m, 4H, Cp), 4.36 (m, 4H, Cp), 7.15 (m, 4H, phenyl H), 7.35 (m, 4H, phenyl H); ^{13}C NMR (C_6D_6) δ 31.6 (CH_3), 34.3 ($C(CH_3)_3$), 38.4 (*ipso*-Cp), 75.2 (Cp), 76.6 (Cp), 119.4 (phenyl CH), 126.5 (phenyl CH), 145.3 (*ipso* phenyl), 150.9 (*ipso* phenyl) ppm; ^{29}Si NMR (C_6D_6) δ −40.8 ppm; MS (EI, 70 eV) *m*/*z* (%) 510 (M^+, 100).

For **4j**: red-orange solid; yield 46%; ^{1}H NMR ($CDCl_3$) δ 4.22 (m, 4H, Cp), 4.71 (m, 4H, Cp), 7.33 (m, 4H, phenyl H), 8.24 (m, 4H, phenyl H); ^{13}C NMR ($CDCl_3$) δ 34.9 (*ipso*-Cp), 74.7 (Cp), 79.3 (Cp), 120.2 (phenyl CH), 126.0 (phenyl CH), 143.2 (*ipso* phenyl), 158.2 (*ipso* phenyl) ppm; ^{29}Si NMR ($CDCl_3$) δ −38.2 ppm; MS (EI, 70 eV) *m*/*z* (%) 488 (M^+, 100).

For **4k**: red-orange solid; yield 52%; ^{1}H NMR (C_6D_6) δ 4.23 (m, 4H, Cp), 4.39 (m, 4H, Cp), 7.15 (m, 8H, phenyl H), 7.39 (m, 10H, phenyl H) ppm; ^{13}C NMR (C_6D_6) δ 38.3 (*ipso*-Cp), 75.6 (Cp), 78.9 (Cp), 120.8 (phenyl CH), 127.1 (phenyl CH), 127.2 (phenyl CH), 128.8 (phenyl CH), 129.0 (phenyl CH), 136.3 (*ipso* phenyl), 140.9 (*ipso* phenyl), 153.3 (*ipso* phenyl) ppm; ^{29}Si NMR (C_6D_6) δ −39.9 ppm; MS (EI, 70 eV) *m*/*z* (%) 550 (M^+, 100).

General Synthesis of Poly(ferrocenylsilanes) 5a−5i, 5k. Polymers **5a**−**5i** and **5k** were prepared similarly, and the general synthesis is illustrated by that of **5a**. To a solution of **4a** (130 mg, 0.47 mmol) in 10 mL of THF under N_2 was added $PtCl_2$ (5 mg, 0.02 mmol). The polymerization reaction was essentially complete after 3 h; however, it was left stirring at room temperature overnight (18 h) and then precipitated into either hexanes or methanol (100 mL). The solution was decanted and dried in vacuo to give **5a** as an amber gum (110 mg, 85% yield).

For polymers **5b**−**5i** and **5k**, methanol was used in the precipitation step.

For **5a**: amber gum; yield 85%; ^{1}H NMR (C_6D_6, 400 MHz) δ 3.65 (s, 6H, OCH_3), 4.43 (m, 4H, Cp), 4.55 (m, 4H, Cp) ppm; ^{13}C NMR (C_6D_6, 400 MHz) δ 51.1 (OCH_3), 66.4 (*ipso*-Cp), 73.0 (Cp), 74.7 (Cp) ppm; ^{29}Si NMR (C_6D_6, 400 MHz) δ −17.2 ppm. Anal. Calcd for $C_{12}H_{14}FeO_2Si$: C, 52.57; H, 5.15. Found: C, 51.80; H, 4.94.

For **5b**: amber gum; yield 83%; ^{1}H NMR (C_6D_6) δ 1.20 (t, $^3J_{HH}$ = 7 Hz, 6H, CH_3), 3.90 (q, $^3J_{HH}$ = 7 Hz, 4H, OCH_2), 4.37 (m, 4H, Cp), 4.50 (m, 4H, Cp) ppm; ^{13}C NMR (C_6D_6) δ 19.1 (CH_3), 59.1 (OCH_2), 67.1 (*ipso*-Cp), 73.1 (Cp), 74.7 (Cp) ppm; ^{29}Si NMR (C_6D_6) δ −20.9 ppm.

For **5c**: amber gum; yield 75%; ^{1}H NMR ($CDCl_3$) δ 4.04 (br m, 4H, OCH_2), 4.16 (m, 4H, Cp), 4.39 (m, 4H, Cp) ppm; ^{13}C NMR ($CDCl_3$) δ 61.6 (q, $^2J_{CF}$ = 35.9 Hz, OCH_2), 62.8 (*ipso*-Cp), 73.5 (Cp), 74.1 (Cp), 124.5 (q, $^1J_{CF}$ = 278.9 Hz, CF_3) ppm; ^{29}Si NMR ($CDCl_3$) δ −13.8 ppm; ^{19}F NMR ($CDCl_3$) δ 56.2 (br m, CF_3) ppm.

For **5d**: reddish gum; yield 88%; ^{1}H NMR (C_6D_6) δ 0.99 (t, $^3J_{HH}$ = 7.1 Hz, 6H, CH_3), 1.54 (m, $^3J_{HH}$ = 7.3 Hz, 4H, CH_2), 1.70 (m, $^3J_{HH}$ = 7.0 Hz, 4H, CH_2), 4.02 (t, $^3J_{HH}$ = 6.4 Hz, 4H, OCH_2), 4.49 (m, 4H, Cp), 4.65 (m, 4H, Cp) ppm; ^{13}C NMR (C_6D_6) δ 14.3 (CH_3), 19.7 (CH_2), 35.5 (CH_2), 63.2 (OCH_2), 67.1 (*ipso*-Cp), 73.0 (Cp), 74.6 (Cp); ^{29}Si NMR (C_6D_6) δ −20.9 ppm.

For **5e**: reddish gum; yield 65%; ^{1}H NMR (C_6D_6) δ 0.96 (m, 6H, CH_3), 1.37 (br m, 8H, CH_2), 1.53 (m, 4H, CH_2), 1.74 (m, 4H, CH_2), 4.05 (t, $^3J_{HH}$ = 6.2 Hz, 4H, OCH_2), 4.52 (m, 4H, Cp), 4.68 (m, 4H, Cp) ppm; ^{13}C NMR (C_6D_6) δ 14.4 (CH_3), 23.2 (CH_2), 26.1 (CH_2), 32.1 (CH_2), 33.3 (CH_2), 63.4 (OCH_2), 67.0 (*ipso*-Cp), 73.0 (Cp), 74.5 (Cp); ^{29}Si NMR (C_6D_6) δ −20.5 ppm.

For **5f**: reddish gum; yield 75%; ^{1}H NMR (C_6D_6) δ 0.97 (t, $^3J_{HH}$ = 6.2 Hz, 6H, CH_3), 1.36 (br m, 32H, CH_2), 1.60 (m, 4H, CH_2), 1.81 (m, $^3J_{HH}$ = 7.0 Hz, 4H, CH_2), 3.90 (t, $^3J_{HH}$ = 6.1 Hz, 4H, OCH_2), 4.54 (m, 4H, Cp), 4.69 (m, 4H, Cp) ppm; ^{13}C NMR (C_6D_6) δ 14.4 (CH_3), 23.2 (CH_2), 26.5 (CH_2), 29.9 (CH_2), 30.0 (CH_2), 30.1 (CH_2), 30.2 (CH_2), 30.3 (CH_2), 32.4 (CH_2), 33.3

(CH_2), 63.5 (OCH_2), 66.9 (*ipso*-Cp), 73.0 (Cp), 74.5 (Cp); ^{29}Si NMR (C_6D_6) δ −20.4 ppm.

For **5g**: amber fibrous solid; yield 70%; ^{1}H NMR (C_6D_6) δ 0.99 (br s, 6H, CH_3), 1.40 (br s, 56H, CH_2), 1.61 (br s, 4H, CH_2), 1.82 (br s, 4H, CH_2), 4.10 (br s, 4H, OCH_2), 4.53 (m, 4H, Cp), 4.69 (m, 4H, Cp) ppm; ^{13}C NMR (C_6D_6) δ 14.4 (CH_3), 23.1 (CH_2), 26.6 (CH_2), 29.8 (CH_2), 30.3 (CH_2), 32.4 (CH_2), 33.5 (CH_2), 63.5 (OCH_2), 67.0 (*ipso*-Cp), 73.0 (Cp), 74.5 (Cp); ^{29}Si NMR (C_6D_6) δ −20.5 ppm. Semicrystalline by WAXS.

For **5h**: amber powder; yield 80%; ^{1}H NMR (C_6D_6) δ 4.09 (m, 4H, Cp), 4.21 (m, 4H, Cp), 6.97 (m, 6H, *para* + *meta* phenyl H), 7.19 (m, 4H, *ortho* phenyl H) ppm; ^{13}C NMR (C_6D_6) δ 64.8 (*ipso*-Cp), 72.9 (Cp), 74.4 (Cp), 119.9 (*para* phenyl), 122.0 (*meta* phenyl), 129.4 (*ortho* phenyl), 154.1 (*ipso* phenyl) ppm; ^{29}Si NMR (C_6D_6) δ −24.2 ppm. Anal. Calcd for $C_{22}H_{18}FeO_2Si$: C, 66.34; H, 4.55. Found: C, 64.83; H, 4.46.

For **5i**: amber fibrous solid; yield 85%; ^{1}H NMR (C_6D_6) δ 1.21 (s, 18H, CH_3), 4.44 (m, 4H, Cp), 4.45 (m, 4H, Cp), 7.16 (m, 4H, phenyl H), 7.35 (m, 4H, phenyl H); ^{13}C NMR (C_6D_6) δ 31.8 (CH_3), 34.3 ($C(CH_3)_3$), 66.0 (*ipso*-Cp), 73.6 (Cp), 75.1 (Cp), 119.9 (phenyl CH), 126.7 (phenyl CH), 144.7 (*ipso* phenyl), 152.7 (*ipso* phenyl) ppm; ^{29}Si NMR (C_6D_6) δ −24.8 ppm. Amorphous by WAXS.

For **5k**: amber fibrous powder; yield 85%; ^{1}H NMR (C_6D_6) δ 4.5 (br s, 8H, Cp), 7.09 (m, 8H, phenyl H), 7.32 (m, 10H, phenyl H) ppm; ^{13}C NMR (C_6D_6) δ 65.7 (*ipso*-Cp), 73.7 (Cp), 75.2 (Cp), 120.8 (phenyl CH), 127.1 (phenyl CH), 127.2 (phenyl CH), 128.8 (phenyl CH), 129.0 (phenyl CH), 136.3 (*ipso* phenyl CH), 140.9 (*ipso* phenyl), 153.3 (*ipso* phenyl) ppm; ^{29}Si NMR (C_6D_6) δ −23.8 ppm. Amorphous by WAXS.

X-ray Structure Determination Technique. Crystals of **4a** and **4j** were mounted on a glass fiber and coated with epoxy glue. Intensity data for both compounds were collected on an Enraf-Nonius CAD-4 diffractometer at 173 K, using graphite-monochromated Mo Kα radiation (λ = 0.710 73 Å). The $\omega-2\theta$ scan technique was applied with variable scan speeds. For each structure, the intensities of three standard reflections were measured every 2 h and corrections were applied when necessary. The data were corrected for Lorentz and polarization effects, and empirical absorption corrections were applied to each data set. The structures were solved by direct methods. Non-hydrogen atoms were refined anisotropically by full-matrix least-squares methods to minimize $\sum w(F_o - F_c)^2$, where $w^{-1} = \sigma^2(F) + g(F)^2$. Hydrogen atoms were included in calculated positions (C−H 0.96 Å). Crystal data, data collection, and least-squares parameters are listed in Table 1. All calculations were performed and graphics created using SHELXTL PC on a PC-486.

Acknowledgment. We would like to thank the Ontario Center for Materials Research for financial support of this work. We also wish to acknowledge the Natural Sciences and Engineering Research Council of Canada (NSERC) for a Postdoctoral Fellowship for P.N. and Postgraduate Scholarships for K.K. and M.M. In addition, I.M. is grateful to the Alfred P. Sloan Foundation for a Research Fellowship (1994−1998), NSERC for an E. W. R. Steacie Fellowship (1997−1999), and the University of Toronto for a McLean Fellowship (1997−2002).

References and Notes

(1) For example, see: (a) Pittman, C. U., Jr.; Carraher, C. E.; Zeldin, M.; Sheats, J. E.; Culbertson, B. M. *Metal-Containing Polymeric Materials*; Plenum: New York, 1996. (b) Pittman, C. U., Jr.; Carraher, C. E.; Reynolds, J. R. In *Encyclopedia of Polymer Science and Engineering*; Mark, H. F., Bikales, N. M., Overberger, C. G., Menges, G., Eds.; Wiley: New York, 1989; Vol. 10, p 541. (c) Chisholm, M. H. *Angew. Chem., Int. Ed. Engl.* **1991**, *30*, 673. (d) Rosenblum, M. *Adv. Mater.* **1994**, *6*, 159.

(2) Manners, I. *Angew. Chem., Int. Ed. Engl.* **1996**, *35*, 1602.

(3) Foucher, D. A.; Tang, B.-Z.; Manners, I. *J. Am. Chem. Soc.* **1992**, *114*, 6246.

(4) Manners, I. *Adv. Organomet. Chem.* **1995**, *37*, 131.

(5) For a novel atom abstraction induced ROP route to poly(ferrocenes) with dichalcogenido spacers see: (a) Brandt, P. F.; Rauchfuss, T. B. *J. Am. Chem. Soc.* **1992**, *114*, 1926. (b) Compton, D. L.; Brandt, P. F.; Rauchfuss, T. B.; Rosenbaum, D. F.; Zukoski, C. F. *Chem. Mater.* **1995**, *7*, 2342.

(6) For ROMP routes to poly(ferrocenes) see: (a) Stanton, C. E.; Lee, T. R.; Grubbs, R. H.; Lewis, N. S.; Pudelski, J. K.; Callstrom, M. R.; Erickson, M. S.; McLaughlin, M. L. *Macromolecules* **1995**, *28*, 8713. (b) Buretea, M. A.; Tilley, T. D. *Organometallics* **1997**, *16*, 1507.

(7) Ni, Y.; Rulkens, R.; Manners, I. *J. Am. Chem. Soc.* **1996**, *118*, 4102.

(8) Ni, Y.; Rulkens, R.; Pudelski, J. K.; Manners, I. *Macromol. Rapid Commun.* **1995**, *16*, 637.

(9) Reddy, N. P.; Yamashita, H.; Tanaka, M. *Chem. Commun.* **1995**, 2263.

(10) Gómez-Elipe, P.; Macdonald, P. M.; Manners, I. *Angew. Chem., Int. Ed. Engl.* **1997**, *36*, 762.

(11) (a) Rulkens, R.; Lough, A. J.; Manners, I.; Lovelace, S. R.; Grant, C.; Geiger, W. E. *J. Am. Chem. Soc.* **1996**, *118*, 12683. (b) Liu, X.-H.; Bruce, D. W.; Manners, I. *Chem. Commun.* **1997**, 289. (c) Petersen, R.; Foucher, D. A.; Tang, B.-Z.; Lough, A. J.; Raju, N. P.; Greedan, J. E.; Manners, I. *Chem. Mater.* **1995,** *7*, 2045. (d) Rulkens, R.; Gates, D. P.; Pudelski, J. K.; Balaishis, D.; McIntosh, D. F.; Lough, A. J.; Manners, I. *J. Am. Chem. Soc.* **1997**, *119*, 10976. (e) MacLachlan, M. J.; Aroca, P.; Coombs, N.; Manners, I.; Ozin, G. A. *Adv. Mater.* **1998**, *10*, 144. (f) Manners, I. *Can. J. Chem.* **1998**, *76*, 371.

(12) Barlow, S.; Rohl, L.; Shi, S.; Freeman, C. M.; O'Hare, D. *J. Am. Chem. Soc.* **1996**, *118*, 7578.

(13) Nguyen, M. T.; Diaz, A. F.; Dement'ev, V. V.; Pannell, K. H. *Chem. Mater.* **1994**, *6*, 952.

(14) Hmyene, M.; Yasser, A.; Escorne, M.; Percheron-Guegan, A.; Garnier, F. *Adv. Mater.* **1994**, *6*, 564.

(15) (a) Nelson, J. M.; Nguyen, P.; Petersen, R.; Rengel, H.; Macdonald, P. M.; Lough, A. J.; Manners, I.; Raju, N. P.; Greedan, J. E.; Barlow, S.; O'Hare, D. *Chem. Eur. J.* **1997**, *3*, 573. (b) Rulkens, R.; Resendes, R.; Verma, A.; Manners, I.; Murti, K.; Fossum, E.; Miller, P.; Matyjaszewski, K. *Macromolecules* **1997,** *30*, 8165. (c) Rasburn, J.; Petersen, R.; Jahr, T.; Rulkens, R.; Manners, I.; Vancso, G. J. *Chem. Mater.* **1995**, *7*, 871.

(16) The influence of different side group substituents on material properties has been well studied for polyphosphazenes and also polycarbosilanes, see: (a) Mark, J. E.; Allcock, H. R.; West, R. *Inorganic Polymers*; Prentice Hall: Englewood Cliffs, NJ, 1992. (b) Rushkin, I. L.; Interrante, L. V. *Macromolecules* **1995**, *28*, 539.

(17) Communication: Nguyen, P.; Lough, A. J.; Manners, I. *Macromol. Rapid Commun.* **1997**, *18*, 953.

(18) Zechel, D. L.; Hultzsch, K. C.; Rulkens, R.; Balaishis, D.; Ni, Y.; Pudelski, J. K.; Lough, A. J.; Manners, I. *Organometallics* **1996**, *15*, 1972.

(19) Wrighton, M. S.; Palazzotto, M. C.; Bocarsly, A. B.; Bolts, J. M.; Fischer, A. B.; Nadjo, L. *J. Am. Chem. Soc.* **1978**, *100*, 7264.

(20) Finckh, W.; Tang, B.-Z.; Foucher, D. A.; Zamble, D. B.; Ziembinski, R.; Lough, A.; Manners, I. *Organometallics* **1993**, *12*, 823.

(21) Israelachvili, J. *Intermolecular & Surface Forces*, 2nd ed.; Academic Press: San Diego, 1994; p 370.

MA980275N